PETROPHYSICAL CHARACTERISTICS OF HOLOCENE BEACHROCK

Baiying Guo* and Gerald M. Friedman
Department of Geology
Brooklyn College of the City University of New York
Brooklyn, New York, 11210
and
Northeastern Science Foundation
Affiliated with Brooklyn College-CUNY,
15 Third Street
P.O. Box 746, Troy, New York, 12181-0746

ABSTRACT: Beachrocks from the Bahamas, Red Sea, Persian Gulf, Mediterranean, southern Caribbean, and Great Barrier Reef (Australia) were classified into six groups on the basis of lithologic and petrophysical characteristics, as follows: Group A--oolitic grainstone, Group B--skeletal grainstone, Group C--packstone, Group D--dolostone, Group E--terrigenous beach-rock, and Group F--Halimeda grainstone. Because for most purposes, groups B and F can be merged, this study recognizes five petrofacies among beachrocks.

Cementation is the diagenetic process exerting the most control over the petrophysical characteristics of the beachrocks. Cements were emplaced progressively. They range from scarce, discontinuous pore-rimming and meniscus cements to one- and two-generation continuous pore-rimming cements, and even to third-generation pore filling. With increasing cementation, porosity decreases significantly. The petrophysical parameters (as shown by the various bivariate plots and capillary-pressure curves obtained through mercury porosimetry) express this decrease. Each of the five beachrock petrofacies possesses consistent petrophysical characteristics. For the most part, the samples tested generated capillary-pressure curves as follows: Groups A, B and F, concave; Group C, intermediate and polymodal; Group D, convex; and Group E, gently sloping and polymodal. With few exceptions, recovery efficiencies relate to porosity. Porosity and median throat size show an approximate positive correlation, but recovery efficiency exhibits an inverse relationship with median throat size.

This study included a prograding sequence of beachrocks from the southern Caribbean. The porosity of the oldest rock (1135±70 years BP) from this sequence is the highest, whereas that of the youngest rock (910±70 years BP) is the lowest.

INTRODUCTION

Mercury porosimetry is widely used in the study of petroleum reservoirs. Data obtained through porosimetry include volume distribution of pore throats, fluid-recovery efficiency, pore-size distribution, and even oil-column height and permeability (e.g., Purcell 1949, Dullien and Dhawan 1974, Schowalter 1979, Wardlaw 1980, Friedman et al. 1981, Jennings 1987, Etris et al 1988, Kopaska-Merkel and Amthor 1988, Wardlaw et al. 1988, Friedman et al 1990). Some authors have found that petrophysical parameters and lithology are related. They have attempted to derive petrophysical classifications related to petrography (Ghosh and Friedman 1989).

Some petrofacies (petrophysical facies) have been classified based on mercury porosimetry analy-

Carbonates and Evaporites, v. 5, no. 2, 1990, p. 223-243

*visiting scholar from Department of Geology, Huainan Mining Institute, Anhui, People's Republic of China

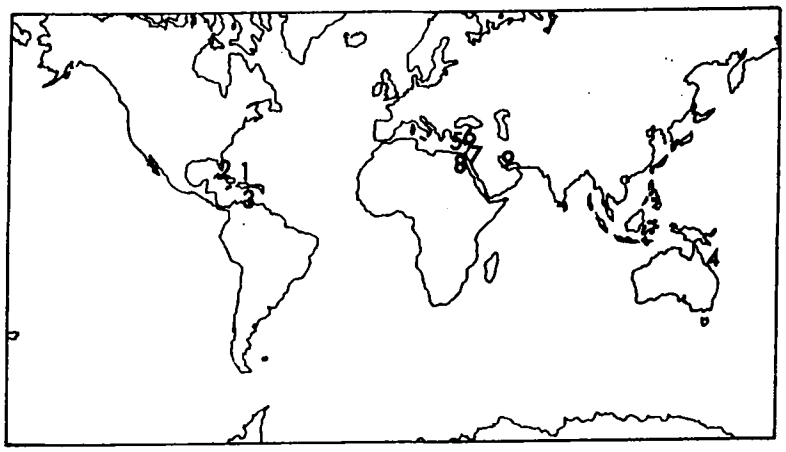

Figure 1. Location map of studied beachrock samples: 1. Bahamas, 2. Florida; 3. Venezuela, 4. Great Barrier Reef; 5. Bardawil, Mediterranean; 6. Kharube, Mediterranean; 7. Gulf of Elat, Red Sea; 8. Gulf of Suez, Red Sea; 9. Persian Gulf.

ses, and interaction of these analyses with lithologic information (Kopaska-Merkel and Friedman 1989). Kopaska-Merkel and Friedman have mapped subsurface units using petrofacies. These mappings could predict the distribution of reservoir- and seal units. Hence, petrofacies study is an important technique in the evaluation of reservoir units.

Previous studies have shown that some lithofacies may belong to different petrofacies because petrofacies were formed largely through diagenesis, which has changed the depositional petrophysical properties of sediments. Accordingly, some questions will be raised: how do petrophysical properties relate to different kinds of original sediments before they were buried? How does diagenesis affect changing pore systems? We hoped that the study of petrophysics of modern cemented rock would provide answers to these questions.

We chose Holocene beachrock for petrophysical study because beachrock represents the first step in the transition from unconsolidated sediment to lithified rock. Beachrock has not been subjected burial diagenesis; its primary pore system is much better preserved than that of ancient rocks. The relationship between the petrophysical properties and lithology of beachrock should actually prove to be more straightforward than that of ancient rocks. It is important to establish modern petrofacies of carbonate rock, such as beachrock, which can then be used to compare with the petrofacies of ancient carbonate reservoir unit.

Of all modern cemented rocks, beachrocks have been studied most extensively. Geologists have studied Holocene beachrocks to determine their mineral compositions, lithologies, cementation, diagenesis, and origin (Ginsburg 1953, Illing 1954, Russell 1963, Stoddart and Cann 1965, Gavish and Friedman 1969, Taylor and Illing 1969, Bricker 1971, Friedman and Gavish 1971, Helsinger 1973, Helsinger and Friedman 1973, Friedman 1975, Krumbein 1979, Flügel 1982, Meyers 1987, Dunkel et al. 1988, Schillings and Richter 1989, Amieux et al. 1989). But, we know of no published reports detailing the petrophysical studies of beachrock.

The purpose of this study was not inquire into the genesis and occurrence of the beachrocks, but into the petrophysical properties of different beachrock lithologies, to relate lithology to pore systems, to find how diagenesis controls pore systems, and to recognize some petrofacies of Holocene beachrock.

This study has shown that the sedimentary environment, sediment properties, and diagenetic history of beachrock have determined the characteristics of both lithology and pore system. Thus, the petrography of beachrocks can be used to predict their petrophysical characteristics.

METHODS

Mercury porosimetry was used for petrophysical analysis of beachrock. In mercury porosimetry, mercury is forced into small voids of rocks. The higher the imposed pressure, the smaller are the voids that are intruded by the mercury. Hence, a graph of cumulative mercury-intrusion volume versus capillary pressure is also a graph of cumulative mercury-intrusion volume versus throat size (Purcell 1949). The following equation expresses the relationship of throat size to pressure:

$$r = \frac{-2\gamma \cos\theta}{P},$$

where:

γ = interfacial tension (485 dynes/cm for Hg/vacuum),

θ = contact angle (130° is used because it is cited most frequently),

P = pressure,

r = the radius of tubular throats.

Because, during near surface diagenesis, neither the particles nor the cement in beachrocks have been extensively recrystallized or deformed, a tubular model of throat shape is appropriate for use with beachrock.

Sampling, cleaning, and experimental procedures follow Ghosh and Friedman (1987), and Kopaska-Merkel and Amthor (1988). Most samples were exposed to pressures up to 20,000 psia.

The intrusion of Hg into some samples ceased at a pressure below 20,000 psia. If this happened, the test run was terminated. In a few samples, intrusion continued to increase at pressures above 20,000 psia. These samples were subjected to pressures up to 30,000 psia. Such high pressures covered the full range of porosity and provided comparison with similar data derived under high pressure for subsurface reservoir rocks (Amthor et al. 1988; Kopaska-Merkel and Friedman 1989).

Several samples were not sufficiently consolidated to permit standard cylindrical core plugs to be made by drilling, but yielded data comparable to that obtained from standard core plugs (see Kopaska-Merkel 1988). Samples were watched closely for any phenomena that might indicate fabric change or damage under high pressure (Amthor et al. 1988). Neither abrupt increase in intrusion at high pressure nor apparent extrusion at decreased pressure were observed. These relationships indicate that, even at high pressures, the samples kept their original fabric.

Traditional petrographic microscopy studies of the samples included the texture of rock, composition of particles and cement, and pore type. The carbonate bomb (Müller and Gastner 1971) was used to determine the concentration of $CaCO_3$ in beachrock containing terrigenous fractions. Staining (Friedman 1959) differentiated aragonite, high Mg-calcite, and low Mg-calcite. X-ray diffraction determined mineralogical composition (Müller 1967, Gavish and Friedman 1973, Milliman 1974).

Location	Number of samples	Lithology	Group
Florida	1	Oolitic grainstone	A
Bahamas 1			
Bimini	1	Skeletal grainstone	B
Joulters Cay	2	Oolitic grainstone	A
Cockroach Cay	1	Oolitic grainstone	A
Schooner Cay	6	Oolitic grainstone	A
Schooner Cay	1	Skeletal grainstone	B
Bahamas 2			
Williams Island	2	Packstone	C
Andros Inland	4	Packstone	C
Mediterranean			
Bardawil	4	Skeletal-peloidal dolostone	D
Kharube	3	Skeletal grainstone	B
Red Sea			
Gulf of Elat	6	Terrigenous beachrock	E
	1	Packstone	C
Gulf of Suez	4	Terrigenous beachrock	E
	2	Oolitic grainstone	A
Australia			
Great Barrier Reef	2	Terrigenous beachrock	E
Southern Caribbean, Venezuela			
Francisqui Cayo	5	*Halimeda* grainstone	F
Vaper Cayo	2	*Halimeda* grainstone	F
Persian Gulf			
Abu Dhabi	1	Oolitic grainstone	A
	1	Packstone	C
	2	Skeletal grainstone	B
Total number of samples	51		

Distribution: Group A: 13; Group B: 7; Group C: 8; Group D: 4; Group E: 12; Group F: 7

Table 1 *LOCATION AND LITHOLOGY OF BEACHROCKS STUDIED*

Radiocarbon dates of two southern Caribbean beachrocks were determined.

PETROGRAPHY OF THE BEACHROCKS

Fifty one Holocene samples were collected from the Bahamas, Red Sea, Mediterranean, Persian Gulf, Great

Cement forms	Description	Porosity (%)	Capillary-pressure curves
Discontinuous pore-rimming	Microcrystalline cement crystals are loosely arranged on surfaces of particles, or meniscus cement fills the corners of pores. Much primary pore space has been preserved. See Figure 2-a.	Primary pores 27.0-32.6	Concave "a" See Figure 9-a
Continuous pore-rimming	More than two generations of cement, commonly the first is dark and cryptocrystalline; and the second, acicular. Occasionally, cement from a third generation fills the remaining pores. See Figure 2-c	Primary pores and few vugs 15.5-19.7	Concave "b" and "c" See Figure 9-b,c
Granular cement	Most of interparticle primary pores are filled by granular calcite cement. Many vugs are formed. See Figure 2-e.	Numerous vugs, less primary 37.7	Bimodal See Figure 10-d

Table 2. THREE CEMENT FORMS RELATED TO POROSITY IN OOLITIC BEACHROCK

lithologic properties, as follows: Group A--oolitic grainstone, Group B--skeletal grainstone, Group C--packstone, Group D--dolostone, Group E--terrigenous beachrock, and Group F-- Halimeda grainstone.

1. Group A--Oolitic Grainstone

Most samples in this group were from the Bahamas (Joulters Cay, Cockroach Cay, and Schooner Cays). The rest were from Florida, the Red Sea, and the Persian Gulf. All of the samples in Group A are white, weakly consolidated, similar-looking rocks. But the samples differ in degree of consolidation and in cement styles. As a result, even among samples belonging to the same lithology and coming from the same environment, petrophysical properties differ.

In general, the rocks of Group A are composed almost entirely of ooids, with ooids constituting more than 95% of their particle volume. Locally, a few skeletal fragments and intraclasts are associated. The diameters of the ooids range from 0.2mm to 1.2 mm; most are 0.3-0.6 mm. They are well sorted and spherical or ovoid in shape. Three kinds of ooids are present: (1) normal, (2) micritized, and (3) superficial (Figure 2-e, a, b).

Cementation: Based on cementation related to porosity, three styles of cement are recognized which affected the porosity of the beachrocks: (1) discontinuous pore-rimming; (2) continuous pore-rimming; (3) granular (Figure 2-a,c,d,e,f; Table 2).

(1) Discontinuous pore-rimming cement includes both discontinuous fringe microcrystalline cement and meniscus cement. In rocks with discontinuous fringe cement, needles of different sizes are loosely arranged on the surfaces of the ooids. The aragonite needles range in length from 2μm to 5μm and may be perpendicular to the surface of the ooids. Much primary pore space is preserved (Figure 2-a). Meniscus cement (Mg-calcite) mainly fills the corners of the pores; e.g., at the contact point of the particles. The effect is to round off the sharp corners (Figure 2-c). So, The rocks with this kind of cement also preserves most of the primary interparticle pores. The clear and transparent crystals of meniscus cements are finely granular, euhedral, and from 6μm to 20μm in size. Rocks with cement type (1) consist of less than 10 percent cement and thus their retained porosities are large (from 27 to 32.6%). These samples occupy the lower right position on the bivariate graph of porosity versus recovery efficiency (Figure 6-b).

(2) Continuous pore-rimming cement. This cement covers particle surfaces continuously and sometimes fills the pores completely; commonly it is composed of two generations. These are cryptocrystalline, thin rim cement (Mg-calcite) covered by acicular aragonite crystals perpendicular to particle surfaces (Figure 2-d). A microcrystalline of Mg-calcite cement may occur between cryptocrystalline and acicular layers. This kind of cement style occupies more than 15 percent of total sample volume and is associated with lower porosities than cement of type (1); porosity ranges from 15.5 to 19.7%. From Figure 6-b, it is clear that by increasing the amount of cement, from discontinuous pore-rimming to continuous pore-rimming cement of two-generation, the porosity is decreased and recovery efficiency is increased.

(3) Granular cement (Figure 2-e). Euhedral to subhedral low Mg-calcite crystals fill most of the interparticle pores. The crystals are 20-60μm in size and are distributed without preferred orientation (Flügel 1982). Also, no pore-rimming cement is

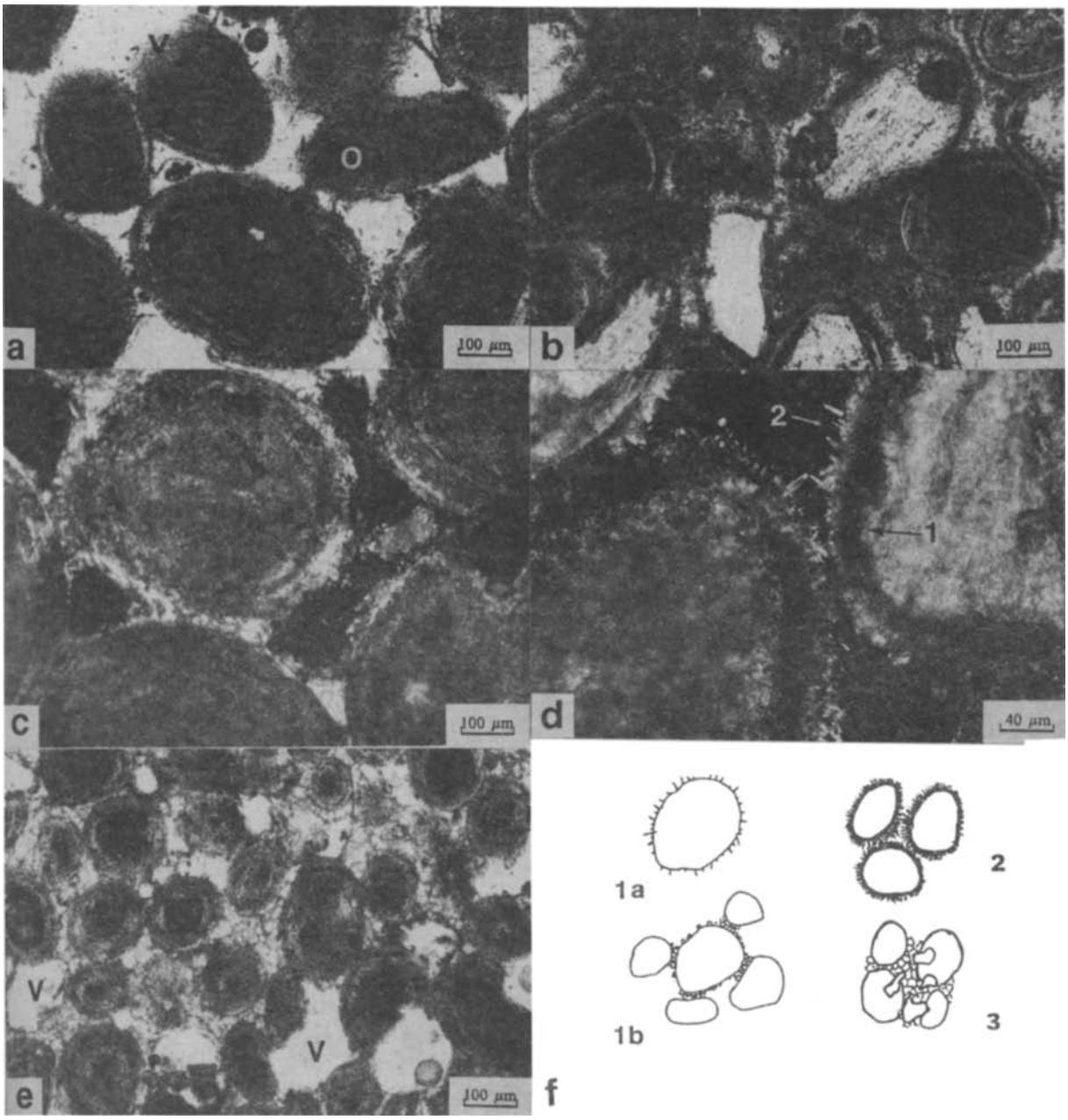

Figure 2. Oolitic beachrock. Photomicrographs, plane-polarized light, except as otherwise noted. a). Micritized ooids, from the Bahamas. Despite the alteration of the nuclei, the thin, concentric laminae are still visible. The boundary between nuclei and concentric laminae is transitional. One ooid (O), at right, retains obscure internal concentric laminae. A little acicular aragonite cement discontinuously rims pores. Some of the ooids (at top left, V) have been partially dissolved, thus increasing the porosity. b). Superficial ooids from Persian Gulf show large nuclei and clear boundaries between nuclei and one or more laminae of coating. c). Microcrystalline meniscus cement from the Bahamas, crossed-polarized light. Pore space is less than "a". The ooid at right bottom displays a tiny intraparticle pore (white area). d). Two-generation continuous pore-rimming cement from the Persian Gulf, crossed-polarized light. The first generation (cement 1) is a thin, dark cryptocrystalline layer (Mg-calcite). The second generation 2 consists of acicular aragonite needles growing perpendicularly to particle surfaces. e). Normal ooids from the Bahamas. Most primary interparticle pores have been filled by granular low Mg-calcite. As a result of dissolution of both ooids and earlier cement, many secondary vugs (v) have formed. f). Sketches of three kinds of cement styles related to porosity in oolitic beachrock. 1a, Discontinuous fringe (see Fig. 2-a) in which acicular aragonite is slightly aligned, and 1b, meniscus cement (see Fig. 2-c); microcrystalline cement was concentrated at the corners of pores. 2, two-generation continuous pore-rimming cement (see Fig. 2-d). By contrast with 1a, acicular aragonite was arranged densely; 3, Granular low Mg-calcite cement with large amount of secondary vugs (see Fig. 2-e).

uted without preferred orientation (Flügel 1982). Also, no pore-rimming cement is observed. This kind of cement, occupying more than 20 percent of sample area in thin sections, was possibly formed by recrystallization of other cement types, such as acicular or cryptocrystalline aragonite/high Mg-calcite. The rock with this cement type is characterized by having many secondary vugs and few primary pores. The sample had more vugs and smaller primary pores than any of the other samples. Porosity of this sample is 37.7%, the highest of all the samples studied. It is located at the upper right on the bivariate graph (Figure 5-a, b), far away from the other oolites. This fact resulted from the special texture and origin. The rock was obviously affected by fresh water after it has been cemented in beach zone.

As mentioned above, the intensity and style of cement strongly controlled the pore system of the oolite beachrock (see discussion).

2. Group B--Skeletal Grainstone

This group includes all grainstones except for oolitic and Halimeda grainstones. A total of 7 samples from the Mediterranean, Persian Gulf, and Bahamas are included in this group. Although all 7 samples are grainstones, different grains, cements, and textures are present.

Three samples from the Mediterranean contain particles of mollusks, brachiopods, and quartz, feldspar, and rock fragments. Most skeletons have been broken but some are perfectly preserved. An important property of the Mediterranean samples is their bedding structure, which results from a parallel orientation of bladed skeletons. In one sample, most of the larger skeletons are convex upward with big shelter pores formed underneath. However, in the other two samples, platy or bladed skeletons are very tightly packed. Accordingly, porosity in these samples ranges from 7.0 to 16.8%. Microcrystals of high Mg-calcite and bladed Mg-calcite are found in these samples, respectively. These cements commonly rim pores or form menisci; in some, they fill pores (Figure 3-a, b).

Grainstones from the Bahamas consist of intraclasts and ooids, and their lithologic characteristics are similar to those of the oolite group. In grainstones of the Persian Gulf, oncolites and intraclasts are found separately. The lithologic properties of these grainstones are diverse. This leads to their different pore systems.

Compared with oolites, both porosity and recovery efficiency are lower. This is because the blade-like shapes of skeletal particles, and their poorer sorting, do not permit packing to be as efficient as in oolites.

3. Group C--Packstone

Eight samples of pellet packstone from the Bahamas were studied. Some calcisiltite and a few skeletal fragments are associated; pellets and peloids occupy from 50 to 80% of the volume of the samples. The pellets and peloids are dark brown, spherical, ovoid or irregular, and their diameters range from 0.05 to 0.2 mm. Commonly the pellets are connected to one another or have even been incorporated into micrite (Figure 3-d). It is possible that these pellets were deposited by biochemical processes as fecal pellets (Friedman and Sanders 1978). Peloids have been observed in place, which present a clear outline, like any grains deposited mechanically (Figure 3-c). Micrite and microcrystalline cement, whose proportion of each sample ranges from 20 to 50% by volume, are important constituent in packstones.

The pores formed between pellets and micrite are of different shapes and sizes. The pellet packstones are characterized by two sizes of interparticle pores, one smaller, the other large than pellets. Pores of the smaller size are ordinary primary interparticle pores, but the larger pores are unusual. Individually, the larger interparticle pores look like fenestrae (Chilingar et al. 1967). However, the shapes and sizes of the larger pores are variable; they are distributed randomly. These large pores are present because cementation stopped compaction of the sediments. Vugs and intraparticle pores can also be seen. Cement, constituting a little more than 15% of the rock, is mainly microcrystalline, rarely needle-form, and is transparent or semi-transparent.

This group possesses the best petrophysical properties of all samples; e.g., high porosities and the highest recovery efficiencies.

4. Group D-- Skeletal-peloidal Dolostone

Four samples were collected from Bardawil, Mediterranean, from the coast of the lagoon. They are classified as dolostone because the main constitu-

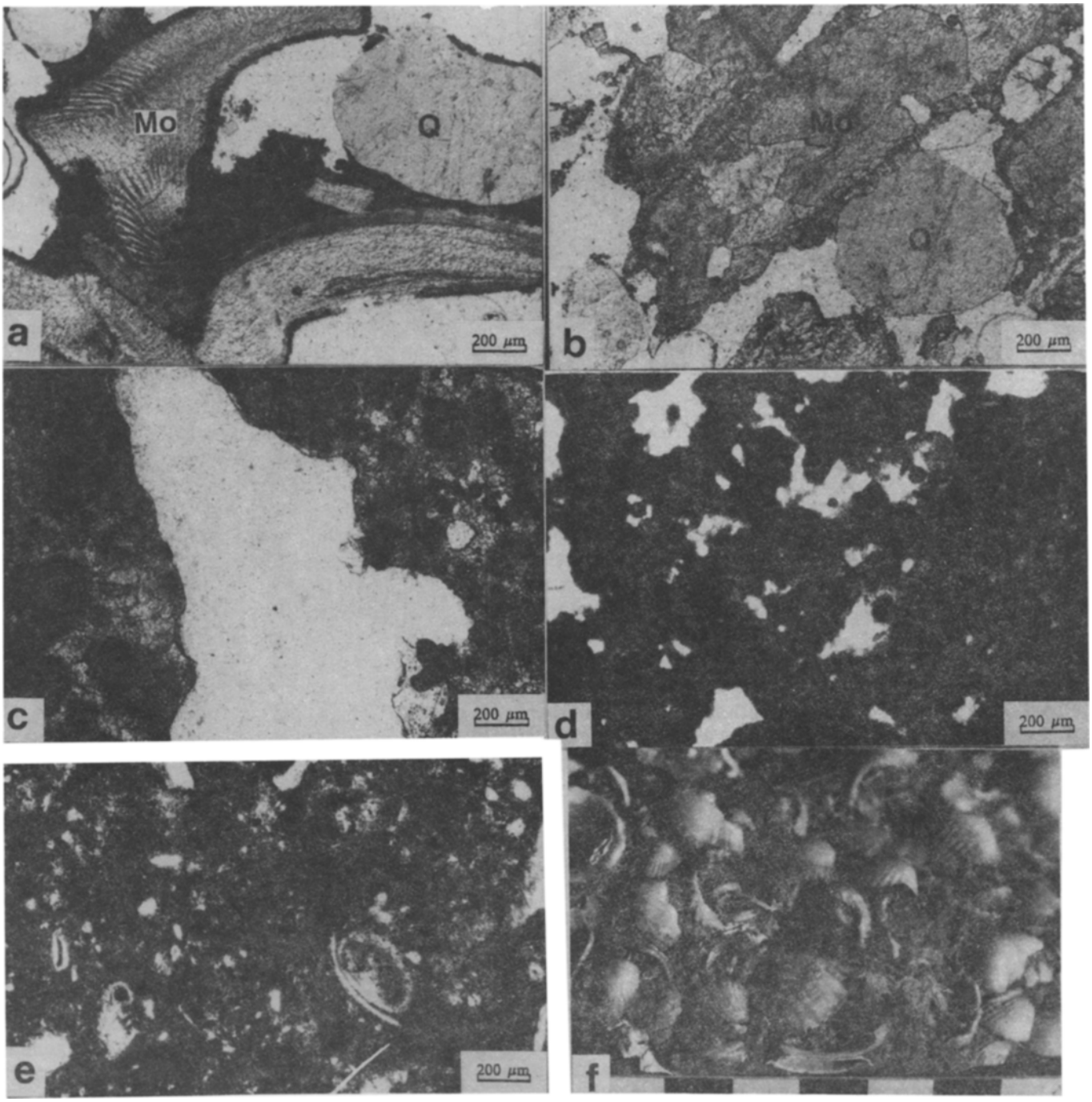

Figure 3. Beachrocks of Group B, C, and D. a). Skeletal beachrock from Kharube, Mediterranean. Particles include mollusk skeletons(Mo) and quartz(Q). Cement is microcrystalline high Mg-calcite (black). Note large remaining interparticle pores (white). b). Skeletal beachrock in which mollusk skeletal debris (Mo) predomnates, Kharube, Mediterranean. Note oriented fabric of elongate skeletal debris in which initial porosity was small compared with Figure 3-a. Bladed Mg-calcite crystals on the particle surface are aligned. c). Peloid-packstone beachrock from the Bahamas. Spaces between peloids are filled by cryptocrystalline cement and tiny skeletal particles. White area at center is a large vug. d). Pellet-packstone beachrock from the Bahamas. Pellets, smaller than peloids in Figure 3-C, have been connected one to another or even incorporated into micrite. Note bimodality in sizes of pores. The large pores look like fenestrae. The diameters of the smaller pores are smaller than those of the pellets. e) and f). Skeletal-peloidal dolostone beachrock from Bardawil, Mediterranean. Photomicrograph "e" shows the fine-textured particle size of sample "f" which consists of molluscan and bryozoan debris, peloids, silt particles and micrite, cement. A few small pores are visible.

Samples	Porosity (%)	Cement (%)	Cementation	Radiocarbon age (year BP)
B51	29.8	8	Cryptocrystalline, equant Mg-calcite	1135±70
B52	20.5	10	Cryptocrystalline, equant Mg-calcite	
B53	17.3	12	First, cryptocrystalline; second, acicular aragonite, >24μm	
B54	13.9	13	Same as B53	
B55	10.7	18	Similar to B53, but lengths of acicular crystals may be more than 30μm. Crystals extend to center of pores.	910±70

From oldest to youngest, porosity and primary pores decrease; cement increases and cementation style changes from one generation to two generations.

Table 3. Relationship of cement and porosity to radiocarbon age in Group F.

ent is dolomite, although texturally, they are wackestones or packstones (Figure 3-e, f). Particles are mainly skeletal and/or peloidal, mixed with a little siliciclastic silts. Mollusks are the most-common skeletal constituents; bryozoans are next in abundance. Most skeletons are 1-2 cm in size, have not been broken, and are well sorted. Other tiny skeletons, such as molluscs and ostracods, and peloidal particles can be identified only under the microscope. Both micrite and microcrystalline cement exist between particles, which consist of dolomite based on x-ray diffraction analysis. The cements have occupied most of interparticle spaces so that primary pores are hardly seen.

5. Group E-- Terrigenous Beachrock (Figure 6-c)

These calcipebblestones and calcisandstones were collected from the northern gulfs of the Red Sea (Gulfs of Elat and Suez) and the Great Barrier Reef of Australia. Most are light brown with reddish tints and are well consolidated; some are weakly consolidated. Terrigenous particles predominate; their diameters range from 0.4 mm to 5 mm, and they consist of rock fragments, quartz, orthoclase, microcline, and plagioclase. The rock fragments, many of which are larger than 2mm, include quartzite, quartz sandstone, basalt, andesite, granite, granite gneiss, calcisandstone, and limestone. Calcareous skeletons are a minor constituent, ranging from 2 to 30%. They include foraminifers, ostracodes, and bryozoans. The particles are well sorted and, because of their coatings, their shapes are sub-rounded or even rounded.

Coated particles can be seen in every thin section from the Red Sea samples, especially on particles less than 3 mm in diameter. Most coarse particles are thinly coated with partial concentric laminae, but on finer particles, the coatings are thick and perfect. In general, quartz particles possess more ideal coatings than do feldspar particles. The thickness of coated layers ranges from 10μm to 60μm. Oolitization always begins from the concave surface of the particles. Because the concentric laminae form on the concave sides of the particles, the particles tend to be subspherical or even spherical (Figure 4-a, b). Every step of oolitization may be observed in thin sections (Figure 4-f). In these samples, steps 1 (partially coated particles) and 2 (superficial ooids) are abundant.

Two types of cement are observed. The first type, which consists of aragonite is 2- or 3-generation cement. The first generation consists of dark cryptocrystalline aragonite rimming the pores. The second generation is formed by transparent acicular aragonite that grew towards the centers of pores (Figure 4-b). After the acicular aragonite had been precipitated, microcrystalline vadose silt filled some residual pores (e.g., Figure 4-c).

The other type of cement is pelletal-cryptocrystalline in form, and is composed of high Mg-calcite. This type is often observed to grade into cryptocrystalline cement through gradual disappearance of the pelletal texture. In some cases, the edges of particles have been dissolved during the cement-precipitation process or were affected by the activity of boring sponges (Figure 4-d).

Almost all pores are primary interparticle; vugs are rare. The porosities of weakly consolidated samples range between 13.8 and 28.3%. The porosities of terrigenous beachrocks that are well consolidated range from 3.6 to 11.3%. Preserved porosity in well-consolidated beachrocks is lower for two reasons: (a) a significant amount of cement formed in multiple generations, and (b) micrite filled most of the residual pore space.

6. Group F-- *Halimeda*-grainstone

Seven samples were collected from southern Caribbean island, off the coast of Venezuela. Again, the lithologic characteris-

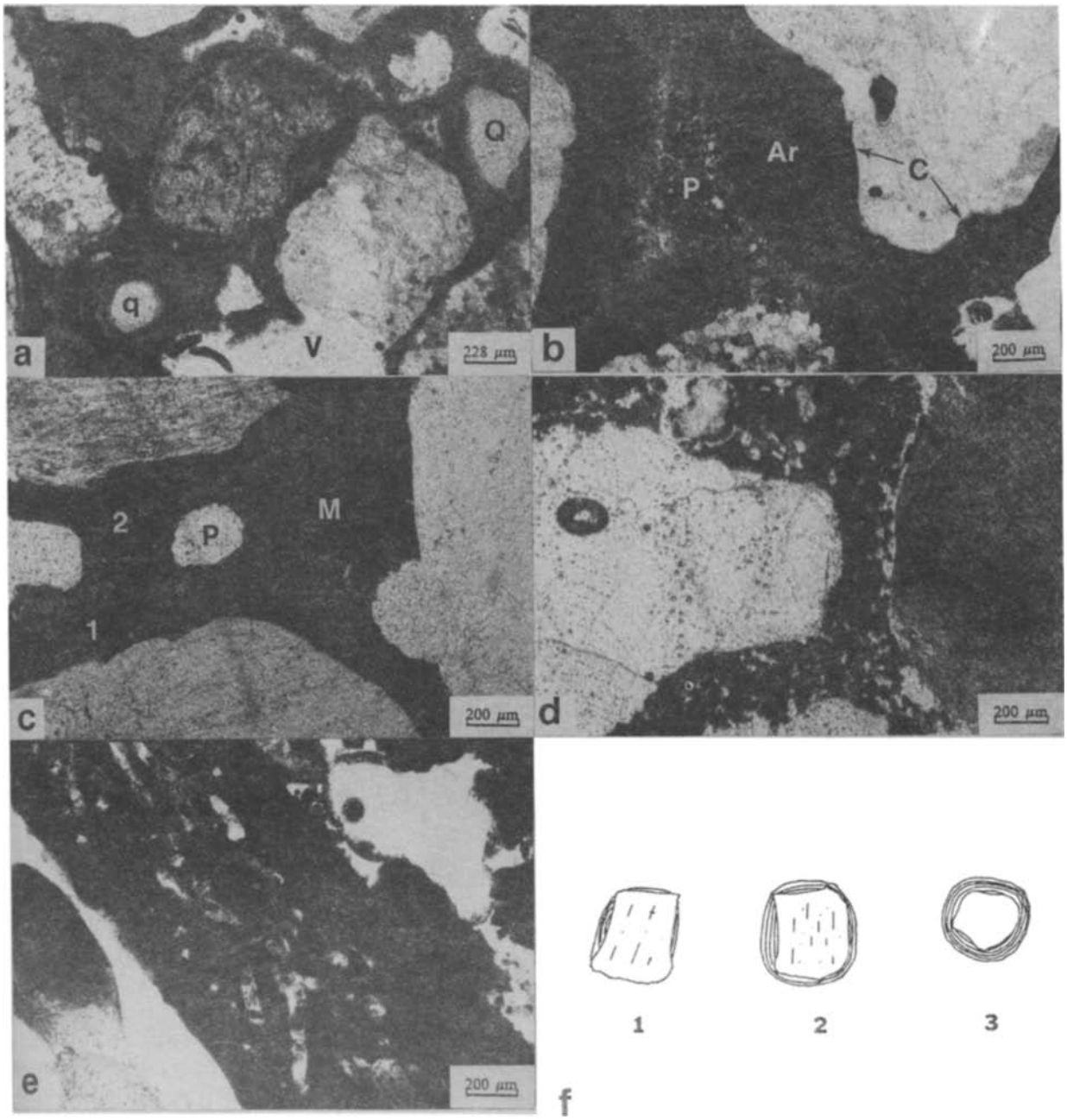

Figure 4. Terrigenous beachrocks, Red Sea area (a,b,c,d), Halimeda beachrock, southern Caribbean (e), and ooid development (f). a). Coated particles in specimen from Gulf of Suez. The coating on the quartz particle (Q) is thicker than that on the feldspar (Pl). The particle at lower left is a normal ooid with quartz nucleus (q). Two-generation cement has obliterated most of the interparticle porosity. At bottom, V is a secondary vug. b). Two-generation cement in specimen from Gulf of Elat, crossed-polarized light. The first cement is dark cryptocrystalline aragonite (Ar); the second, transparent acicular aragonite. Only a small triangular primary pore is preserved (P). Note oolitized coating (dark gray, C) has formed on the concave surface of the grain at the right top. c). Two-generation cement in specimen from Gulf of Elat. After the two generations (1 and 2) of cement had formed, dark vadose silt (M) filled most of remaining pores so that only a small pore (P) is preserved. d). Pelletal-cryptocrystalline cement from Gulf of Elat. High-Mg calcite cement occupies most primary interparticle pores. e). Halimeda grainstone beachrock from southern Caribbean. Partial section of a Halimeda particle, showing dark calcified plates with abundant irregular holes that were originally filled with organic matter. A large proportion of the primary porosity has been preserved. f). Sketches of the stages of oolitization. 1, partially coated particle; 2, superficial ooid; and 3, normal ooid. Further description in text.

Group	Porosity (%)	Recovery efficiency (%)	Median throat size (microns)	Normalized throat size	Numbers of sample
A	24.22* 15.52-37.69	21.30 7.91-42.67	15.69 0.47-33.17	6.19 0.9-50.60	13
B	17.79 7.01-23.34	20.48 4.20-35.80	12.37 2.59-19.16	2.81 1.88-4.13	7
C	22.72 18.63-26.20	42.71 28.20-56.30	1.7 0.14-6.38	6.12 0.68-15.52	8
D	4.16 3.07-5.35	9.66 3.23-15.71	0.01 0.01-0.015	65.14 12.40-202.4	4
E	12.11 3.63-26.94	20.98 9.52-36.08	7.45 0.15-26.95	15.96 1.64-99.47	12
F	17.19 10.70-29.75	29.32 11.88-63.83	11.35 0.48-26.81	2.96 1.25- 5.83	7

* 24.22 (average) = 15.52-37.69 (minimum-maximum)

Table 4. PETROPHYSICAL DATA OF BEACHROCK

tics of the samples are similar, but their petrophysical properties are different. Five of these samples form a prograding sequence from B51 (oldest), to B55 (youngest) (Table 3; Figure 5).

The particles consist mainly of the green alga, *Halimeda*, accounting for 60% (point counting). Coral fragments follow with 27% on average. Red alga (possibly *Lithophyllum*), mollusks, foraminifera, and echinoderms are less common. Variable sections of *Halimeda* are perfectly preserved, as seen under the microscope (Figure 4-e). *Halimeda* debris consists of dark calcified plates with abundant irregular holes that were originally filled with organic matter; intercept areas of individual particles average 0.5 x 2 mm. Broken coral particles displaying fibrous biocrystalline texture average 0.4 mm in size.

From oldest to youngest in the prograding sequence, the quantity of cement increases and its style changes, from an early equant Mg-calcite cryptocrystalline cement, to a two-generation cement consisting of an equant cryptocrystalline cement covered by an acicular aragonite rim cement. Correspondingly, porosity declines from 29.8 to 10.7% and the sizes of primary pores decrease. This significant change of porosity occurred over the course of only 225 years. Obviously, porosity in these samples is controlled by the quantity of cement.

A possible cause for increasing cementation with age is a rapid epeirogenic rise of the island. The oldest unit escaped cementation because of rapid emergence. In contrast, the younger unit were kept in contact with sea water for a longer time and hence were subject to longer periods of cementation.

This sequence suggests that among all diagenetic processes affecting beachrocks, cementation is the most-significant process in reducing porosity.

PETROPHYSICS OF BEACHROCKS

Many important petrophysical parameters of reservoirs related to their pore systems are derived from porosimetry. Of these parameters, porosity, recovery efficiency (RE), median throat size, normalized throat size, and kind of capillary-pressure curve are regarded as the most significant (Amthor et al. 1988, Ghosh and Friedman 1989, Jennings 1987, Kopaska-Merkel and Amthor 1988, Kopaska-Merkel and Friedman 1989, Wardlaw 1976, Wardlaw and McKellar 1981, Wardlaw et al. 1988).

Porosity

The porosity of the beachrocks varies greatly from one group to another. Even among samples collected from the same area and of the same lithology, significant differences in porosity exist. We attempted to discover what porosities characterize beachrocks, how many porosity ranges and what kinds of pores exist, as well as how lithological properties control the porosity of beachrocks.

From Table 4 and Figure 8-a, we know Group--A (oolitic grainstone) possesses the highest average porosity of all groups - 24.2%. The porosity of Group--C (pellet packstone) is 22.7%; followed by Group--B (skeletal grainstone), 17.8%; Group--F (Halimeda grainstone), 17.2%; Group--E (terrigenous beachrock), 12.1%. The least-porous group is Group--D (dolostone); on the average, its porosity is only 4.2%.

Factors Controlling the Porosity of Beachrock: The porosities of the sediment matrix, the sedimentary environment, and diagenetic processes affect the pore systems of rocks.

Compared with other grainstones, the largest primary interparticle pores have been preserved in oolites because of their high particle sphericities and good sorting. In pellet packstones, two kinds of primary interparticle pores are present. One is smaller than the pellets, whereas the other, which formed between micrite particles and/or pellets, is larger than the pellets. These large pores resemble fenestral pores, and are responsible for the high porosities of the wackestones, which are greater than the porosities of the grainstones studied. Terrigenous beachrocks are less well sorted and initially packed tightly. Therefore, they have retained lower porosities. In summary: shape, size, sorting of sedimentary particles, and their arrangement or packing style determined the primary porosity. The primary pores created by the deposition of sediments are the predominant pore type in beachrocks.

Sedimentary environments control the properties of sediments, including those found in beachrocks. For example, every sedimentary realm contains a predominant particle type. Further, samples of a single lithology collected from areas with differing sedimentary environments may possess different porosities (e.g., terrigenous Group, Figure 6-c) - the porosity of sandstones from the Gulf of Suez is much greater than that of those from the Gulf of Elat although both gulfs are northern extension of the Red Sea. Finally, consider the dolostone of Group D. This rock formed in an unusual environment near a sea-marginal lagoon. As a result of dolomitization, the porosity of this beachrock is very low.

Diagenesis is an important controlling factor for porosity. The beachrocks described here were consolidated principally by cementation. The effects of compaction were negligible. The oolitic group (Group A) illustrates how porosity is controlled by cementation (Figure 6-b). Rocks with high

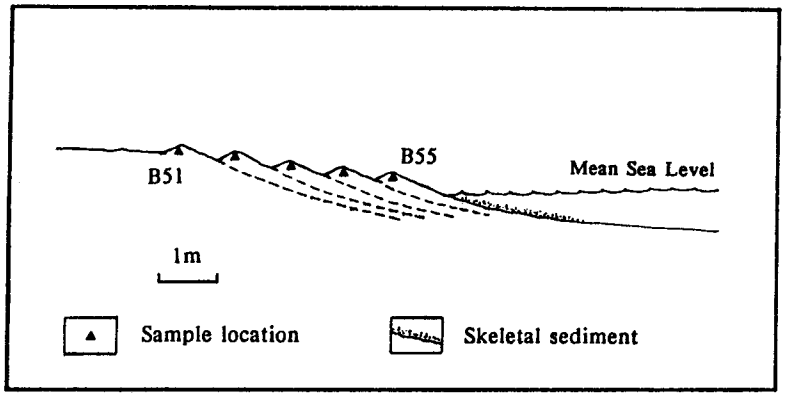

Figure 5. Profile sketch of Halimeda beachrock of prograding sequence from Francisqui Cayo, southern Caribbean. Vertical scale is exaggerated. Oldest layer (B51) is located landward and youngest (B55) seaward.

porosities (generally more than 25%), are weakly cemented with discontinuous fringe and/or meniscus cement. Well-cemented rocks with continuous pore-rimming and/or two-generation cement are less porous (porosity commonly less than 20%). Consequently, as cement increases, porosity decreases.

Dissolution or boring was a significant factor locally, as in a sample from Bahama, whose porosity is the highest of all samples described here. In this rock, vugs are the dominant pores and primary interparticle pores are less important.

Similarly, on the basis of consolidation, the terrigenous beachrock group (Group E) can also be subdivided into subgroups. One subgroup, showing less porosity, has been well consolidated; it contains two or three generations of cement. The other, which is much more porous, is weakly consolidated and contains little cement (Figure 6-c).

Porosity Related to other Petrophysical Parameters (Table 5): Data on the relationship of porosity to recovery efficiency from research on reservoir rocks are divergent (Wardlaw and Taylor 1976, Wardlaw 1976 and 1980, Amthor et al. 1988, Kopaska-Merkel and Friedman 1989). In this study, porosity is roughly proportional to recovery efficiency (RE) for all samples (Figure 7-b). Correspondingly, on the bivariate graph of porosity versus RE, most groups show a positive relationship (Figure 6-c, d, 8-a), but Group A (oolite grainstone, Figure 6-a) and Group F (Halimeda grainstone) do not. Although Wardlaw (1976 and 1980) explained the changing relationship between porosity and RE by different pore geometry, it is not clear whether this interpretation is valid for these beachrocks.

Considered as a whole, a positive relationship between porosity and median throat size exists for all samples (Figure

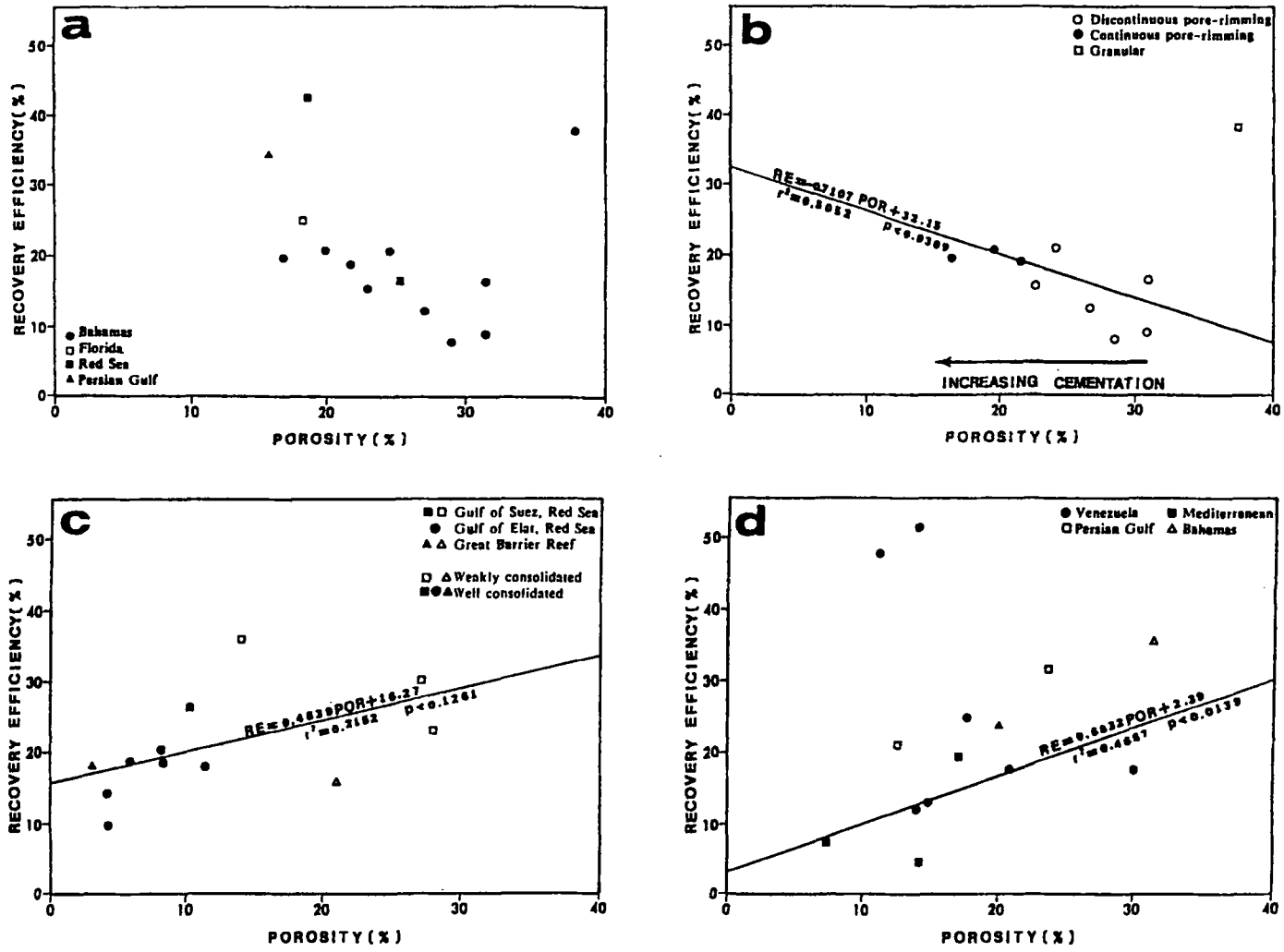

Figure 6. Graphs of recovery efficiency (RE) vs. porosity. a). 14 samples of group A are from Bahamas, Florida, Red Sea, and Persian Gulf. Porosity is inversely proportional to RE. b). Bahamas oolitic beachrocks. Graph shows discontinuous pore-rimming cement, continuous pore-rimming cement, granular cement. The line and formula in the graph express the multiple regression results. Porosity is related to cement type. c). Group E--terrigenous beachrock. Samples are from Gulf of Suez, Red Sea, the Great Barrier Reef, and the Gulf of Elat, Red Sea. The graph shows that petrophysical properties are controlled by the degree of consolidation or cementation. The well-consolidated samples with more cement exhibit smaller porosity and RE. Porosity is a positively related to RE (based on multiple-regression statistics). d). Group B and Group F. Samples are from southern Caribbean (Venezuela), Mediterranean, Persian Gulf, and the Bahamas. These samples are all grainstones, but display divergent porosities and recovery efficiencies, because they are of a different grain type and texture, and originated in different areas. RE and porosity are positively related.

7-b). However, groups B and C display a negative relationship, and groups D, E and F show no clear relationship between porosity and median throat size.

Recovery Efficiency

Recovery efficiency (RE) is the percentage of trapped hydrocarbons which may be withdrawn from a reservoir rock under a particular set of conditions. In mercury porosimetry, RE is the percentage or fraction of mercury intruded at maximum pressure which is extruded during pressure reduction to final minimum pressure (14-15 psia or atmospheric pressure)

The mean recovery efficiency of each group is shown in Table 4. The RE values of the packstone group are the highest. The Halimeda grainstone group is next. Groups A, B, and E yielded similar RE values. Group D (dolostone) had the lowest RE

Group	Parameters	Recovery efficiency	Median throat size	Normalized throat size
A		-	+	
B		+	-	
C	Porosity	+	-	
D		+	?	
E		+	?	
F		-	?	
Total		+	+	
A			-	?
B			-	?
C	Recovery		-	-
D	efficiency		-	?
E			?	-
F			-	?
Total			-	-

+ represents positive relationship

- mean inverse relationship

? relationships are not clear

Table 5. RELATIONSHIPS AMONG PETROPHYSICAL PARAMETERS OF BEACHROCKS

values. This can also be seen from Figure 8-a.

Clearly, recovery efficiency is inversely proportional to median pore-throat size both for each group and for all samples (Figure 8-b & 7-c). The data are consistent with previous work (Wardlaw 1976, Amthor et al. 1988, Kopaska-Merkel and Friedman 1989).

Median Throat Size

In order from largest to smallest median throat size, the groups are: A, B, F, E, C, and D. Group D is an exception to the general trend, having both low RE values and small median throats; the RE values of group C are the highest .

Normalized Throat Size (NTR)

Many previous workers paid much attention to the sorting of throat size and took it to exert a strong affect on recovery efficiency. Normalized throat size represents throat-size sorting (Wardlaw et al. 1988, Kopaska-Merkel and Friedman 1989).

Normalized throat size =

$$\frac{\text{(throat size 20\% - throat size 80\%) mercury saturation}}{\text{throat size at 50\% mercury saturation*}}$$

Curve type		Porosity	Recovery efficiency	Median throat size	Normalized throat size	Low-pressure intrusion	High-pressure intrusion
Concave	a	High	Low	Large	Low	Large	Small
	b	|	|	|		|	|
	c	Moderate	Moderate	Moderate		Moderate	Moderate
Convex		Low	Low	Very low	High	Low	Moderate
Gently sloping		Low	Low	Low	Moderate --high	Low ------>	Moderate
Intermediate		High	High	Low	Low	Low	High
Polymodal				Variable			

Table 6. CATEGORIES OF CAPILLARY-PRESSURE CURVES OF THE BEACHROCKS

* throat size 20% means the throat size that is measured from the incremental capillary-pressure curve when 20% of the maximum intrusion volume has occurred.

Figure 7-d and Table 4 present the characteristics of normalized throat size in the beachrocks. First, the average values of each group are very different and therefore, they are separated widely on Figure 7-d. Second, a general inverse relationship exists between RE and normalized throat size for all samples. This relationship is not clear within individual groups because values for normalized throat size among the samples of each group are similar.

Capillary-Pressure Curves

Five kinds of capillary-pressure curves are classified (Table 6). This classification is derived from that of Amthor et al. (1988), but with two important differences. First, convex curves are associated with low RE values. The extrusion curves are not subparallel to intrusion curves for this convex capillary-pressure curves. So, this kind of curve is different from any documented by Amthor et al. (1988). Second, we found a series of concave curves that can be subdivided into three sub-categories based on the shapes of the curves and the intrusion volumes under high pressure. The distribution of each kind of capillary-pressure curve in each group of beachrock is shown in Table 7.

(1) Concave Curves: Most samples of groups A, B, and F, and one samples of group E, 28 in all, yield concave curves (Table 7). Compared with other curves, concave curves coincide with higher porosities, moderate recovery efficiencies, higher intrusion under low pressure and low- to moderate intrusion at

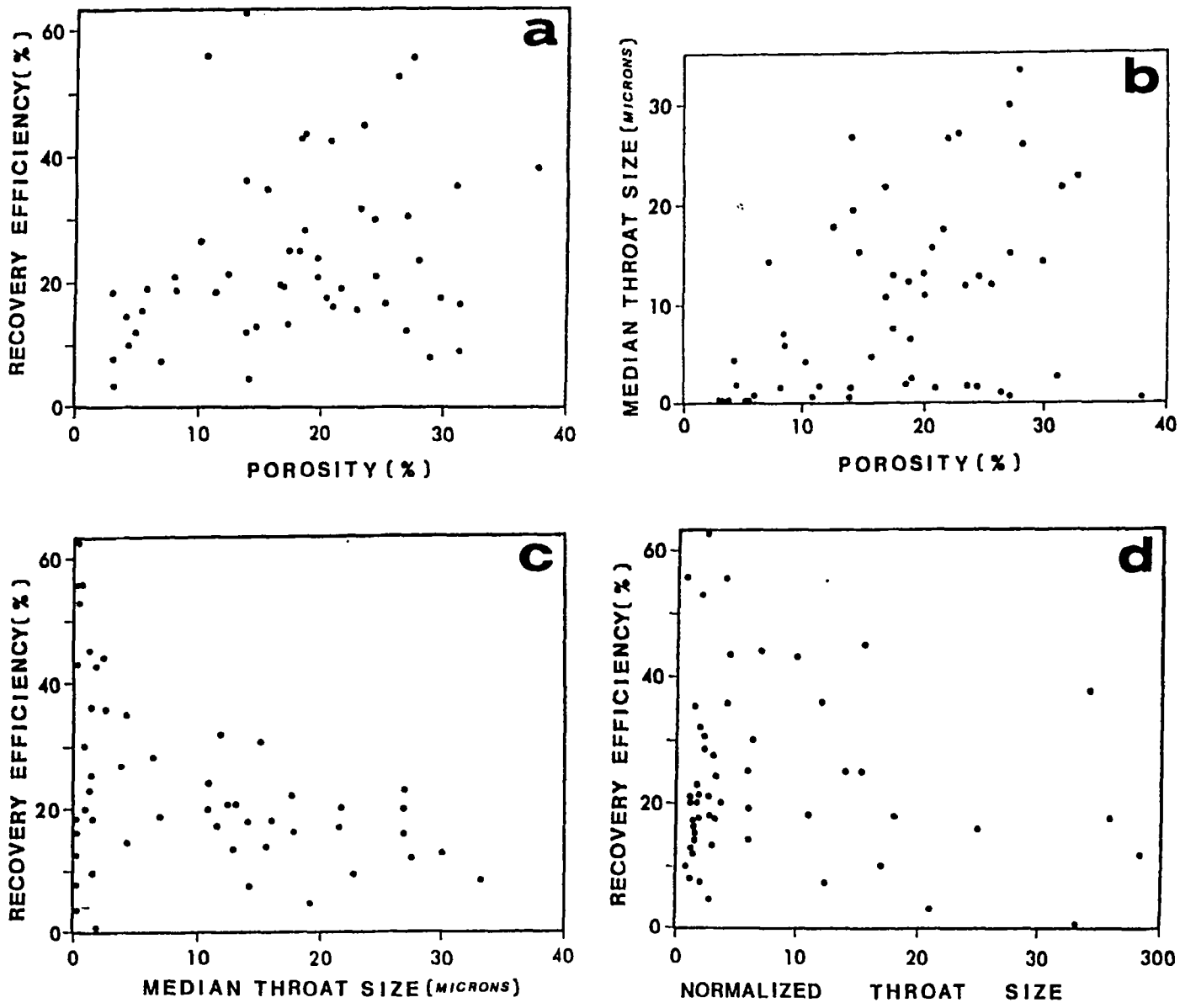

Figure 7. Bivariate plot of all studied beachrock samples. a). Bivariate plot of recovery efficiency versus porosity; a weak positive relationship is indicated between RE and porosity. b). Bivariate plot of median throat size versus porosity shows an approximate positive relationship between them. c) Bivariate plot of recovery efficiency versus median throat size. An obvious inverse relationship exists between them. d). Bivariate plot of recovery efficiency versus normalized throat size; a weak inverse relationship exists between RE and normalized throat size. Note that the normalized throat size of most samples is less than 10.

high pressure. According to the shapes of incremental curves and the amounts of intrusion at high pressure, three sub-categories of concave curves are recognized (Figure 9-a, b, c,).

Concave "a" curves are steep and indicate little intrusion at high pressure. Samples with concave "a" curves possess larger median throats and lower recovery efficiencies compared to samples with concave "c" curves. The slope of concave "c" curves are gentle and indicate moderate intrusion under high pressure. Thus the median throats of samples having concave "c" curves are smaller, and their RE values are higher. Concave "b" curves are intermediate.

This classification corresponds well to petrographic information. The samples of Group A in which the cement is discontinuous (such as sample

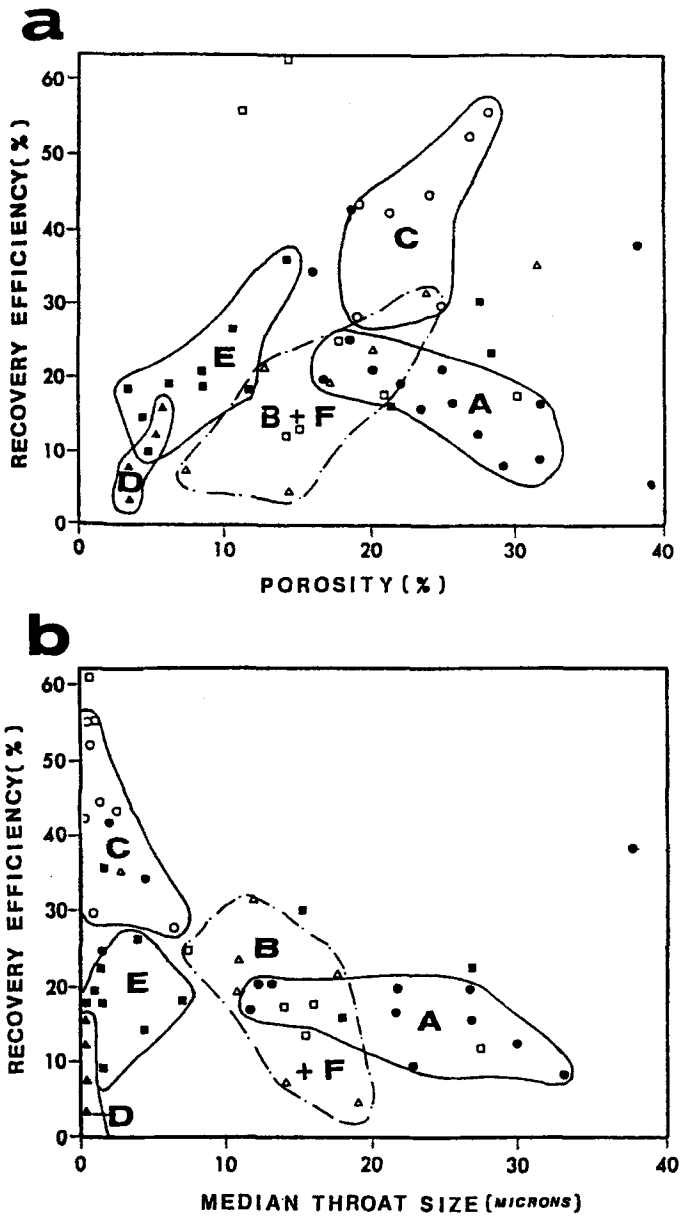

Figure 8. Bivariate plots of (a) recovery efficiency and porosity, and (b) recovery efficiency and median throat size for beachrocks of five different kinds of petrographic- and petrophysical characteristics, as follows: Group A (oolitic grainstone petrofacies from Bahamas, Red Sea and Persian Gulf), Group B and F (skeletal grainstone petrofacies from Mediterranean and southern Caribbean, Venezuela), Group C (pelletal packstone petrofacies, Bahamas), Group D (dolostone petrofacies, Mediterranean lagoon), and Group E (carbonate-cemented terrigenous petrofacies, Red Sea). Filled circle--Group A, open circle--Group C, filled square--Group E, open square--Group F, open triangle--Group B, filled triangle--Group D. Note that, in both plots, groups A, C and E are distinct from each other, whereas groups D and B+F overlap other groups.

Group	Concave a	Concave b	Concave c	Convex	Gently sloping	Inter-mediate	Polymodal
A	3	4	5				2
B	1	5	1				
C	1	1				2	3
D				4			
E			1		7		4
F		2	4				1
Subtotal	4	12	12				
Total		28		4	7	2	10

Table 7. NUMBER OF CAPILLARY-PRESSURE CURVES OF EACH KIND IN EACH GROUP OF THE BEACHROCKS

B36) yield curves of sub-category concave "a". As the amount of cement increases (one- or two-generation continuous pore-rimming), and porosity and median throat size decrease, concave "a" curves are replaced by concave "b" or, even concave "c" curves.

(2) Convex Curves: (Figure 10-a): Only four samples of Group D show convex curves and they are from Bardawil, Mediterranean. The porosities and recovery efficiencies of these samples are low; median throat sizes are small. Their normalized throat sizes are large. These convex curves differ from those of Amthor et al (1988).

(3) Gently sloping curves (Figure 10-b): We have seven samples with gently sloping curves, which are from Group E (terrigenous beachrocks). They are characterized by low porosities, low RE values, and small median throats but moderate- to high normalized throats.

(4) Intermediate curves (Figure 10-c): Only two samples, pellet packstones of Group C from the Bahamas, are assigned to this type. They are characterized by good "sorting" of throat size and a leptokurtic throat-size distribution. They keep high RE values, relatively high porosities, small median throats and small normalized throats. This is the "ideal" curve for reservoir rocks.

(5) Bimodal and polymodal curves (Figure 10-d): Ten samples in groups E, C, A, and F belong to the bimodal- or polymodal types. Actually, the curves of many of these samples are intermediate between concave- and typical polymodal curves. Their throat-size distribution shows more than one peak and their cumulative curves are more or less "S"-shaped. The samples with polymodal curves

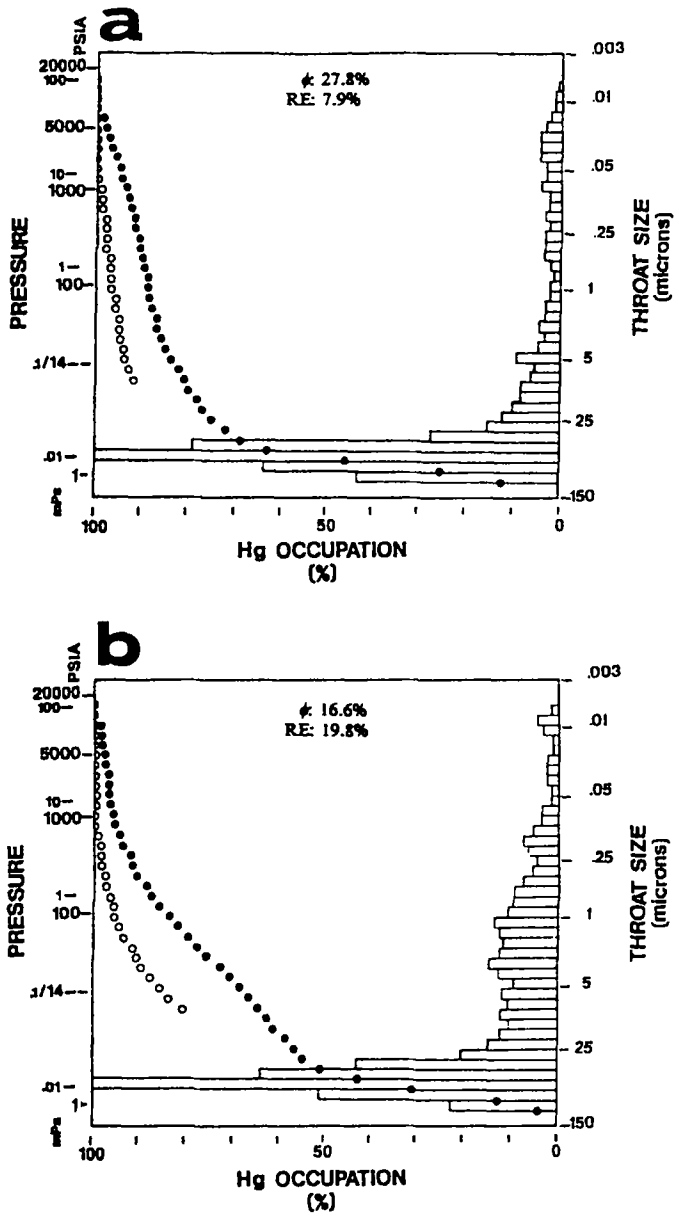

Figure 9. A series of concave capillary-pressure curves for oolitic grainstone (Group A). Filled circles represent cumulative mercury intrusion curve; open circles represent extrusion; open bars of histogram show incremental intrusion. u: porosity; RE: recovery efficiency.

a). Graph for Bahamas oolitic. Note steep slope of curve and small RE. At high pressures, only a little mercury has been intruded. The samples with this kind of capillary-pressure curves occured discontinous pore-rimming cement.

b). Graph for Bahamas oolitic beachrock. Note decreasing slope, more intrusion at high pressure and larger RE compared with figure 9-a. The samples present thin continous pore-rimming cement.

c). Graph for Red Sea oolitic beachrock from Gulf of Suez. Note gently sloping intrusion curve. Compared with Figures 9-a and 9-b, it presents the largest intrusion at high pressure and the largest RE. The samples possess two-generation continous pore-rimming cement.

present variable petrophysical characteristics, which often depend on what group they belong to.

In summary, the shapes of the incremental- and cumulative-intrusion curves for each group of beachrocks are characteristic. Most samples of groups A, B, F (all grainstones but with different particle types) are concave. Group D yields special, convex curves. Most of the curves of Group E are gently sloping, although a few samples yield polymodal curves. Group C curves are intermediate and polymodal (Table 7).

DISCUSSION

Although the petrophysical characteristics of the beachrock vary, the lithologic and petrophysical properties are related. First, we found that the petrophysical parameters of each group are distinct from those of the others (Table 4). Second, on bivariate graphs, samples collected from the same environment (or realm) and of similar lithologic nature plot close to each other (Figure 8-a, b). On these graphs, samples of group A, C, and E always occupy different areas although Group D and group B+F overlap with others. Finally, each group possesses its own specific type of capillary-pressure

curve (Table 7). These findings uphold the conclusion that environment and lithologic characteristics exert substantial control on petrophysical properties; diagenesis is a secondary, but quite important factor.

Because the lithologic characteristics and petrophysical properties of samples from a single group are similar, they may be assigned to a common petrofacies (Kopaska-Merkel and Friedman 1989). Groups B and F exhibit similarity in characteristics (Table 4, Figures 8-a, b) such that it is appropriate to merge them into a single petrofacies. Hence, among the samples studied, five petrofacies are recognized (Table 8).

Petrofacies can be distinguished by both the kinds of capillary-pressure curves and the bivariable plots of petrophysical parameters (Table 8 and Figure 8). Oolitic and skeletal grainstone petrofacies present concave curves; packstone petrofacies, intermediate and polymodal; dolostone petrofacies, convex curves; terrigenous beachrock petrofacies, gently sloping and polymodal curves.

A few samples lie outside the groupings of Figure 8 to which they should belong. This results from the different sampling localities, and the variability of the petrophysical properties of the beachrock studied. However, for almost all of the samples, membership in the same petrofacies implies similar, consistent petrophysical characteristics.

We also note that the both oolitic grainstone petrofacies and the skeletal grainstone petrofacies possess concave curves, and, in the bivariable plots, they are overlapped. The reason for this is that in skeletal grainstone group, there are various kinds of grains such as skeletal, oolitic, intraclastic, etc., so that some of samples of the skeletal grainstone group have similar lithologic and petrophysical properties to the oolitic group. But the oolitic group is characterized its own nature as mentioned before.

Petrofacies	Group	Lithology	Porosity	RE	Capillary-pressure curves
Oolitic grainstone	A	Oolitic grainstone	Highest	Low-moderate	Concave
Grainstone	B & F	Skeletal & intraclast grainstone	Moderate	Variable	Concave
Wackestone	C	Pelletal packstone	High	Highest	Intermediate Bimodal
Dolostone	D	Skeletal-peloidal dolostone	Low	Low	Convex
Terrigenous	E	Sandstone, granule-stone	Moderate -low	Low	Gently sloping Polymodal

Table 8. PETROFACIES OF THE BEACHROCKS

CONCLUSIONS

1. Beachrocks from different realms possess divergent petrophysical properties resulting from their different sedimentary environments, lithologies, and diagenetic histories. In all of these, lithology is a first controlling factor. lithofacies and petrophysics of beachrocks are related. Even though there is some variation of petrophysical properties among the samples of each group, the properties of a groups's samples are still proximate when contrasted with those of samples from other groups. Five petrofacies are recognized; e.g., oolitic and skeletal grainstones, packstone, dolostone and terrigenous beachrocks.

2. In beachrocks, cementation has been the most-important diagenetic process. It commonly controls the evolution of the pore system. In oolite and Halimeda beachrocks, as cementation progresses (from scarce, discontinuous pore-rimming cement to one- and two-generation continuous pore-rimming cement), porosity and median throat size decreases but recovery efficiency increases. Meanwhile, with increasing cementation, capillary-pressure curves change from concave "a" to concave" c".

3. A prograding sequence of beachrocks from islands off the coast of Venezuela was included in this study. The beachrocks exhibit regular beds dipping gently seaward, with the oldest bed farthest from the sea. All five Venezuelan samples are lithologically similar, but differ in cement type and cement quantity, with resulting differences in pore systems. As the age of the beds decreases, their porosity drops from 29.8 to 14.6%; RE increases from 17.2 to 63.8%; and median throat size is reduced from 13.9 μm to 0.5 μm. This sequence displays porosity that is directly proportional to

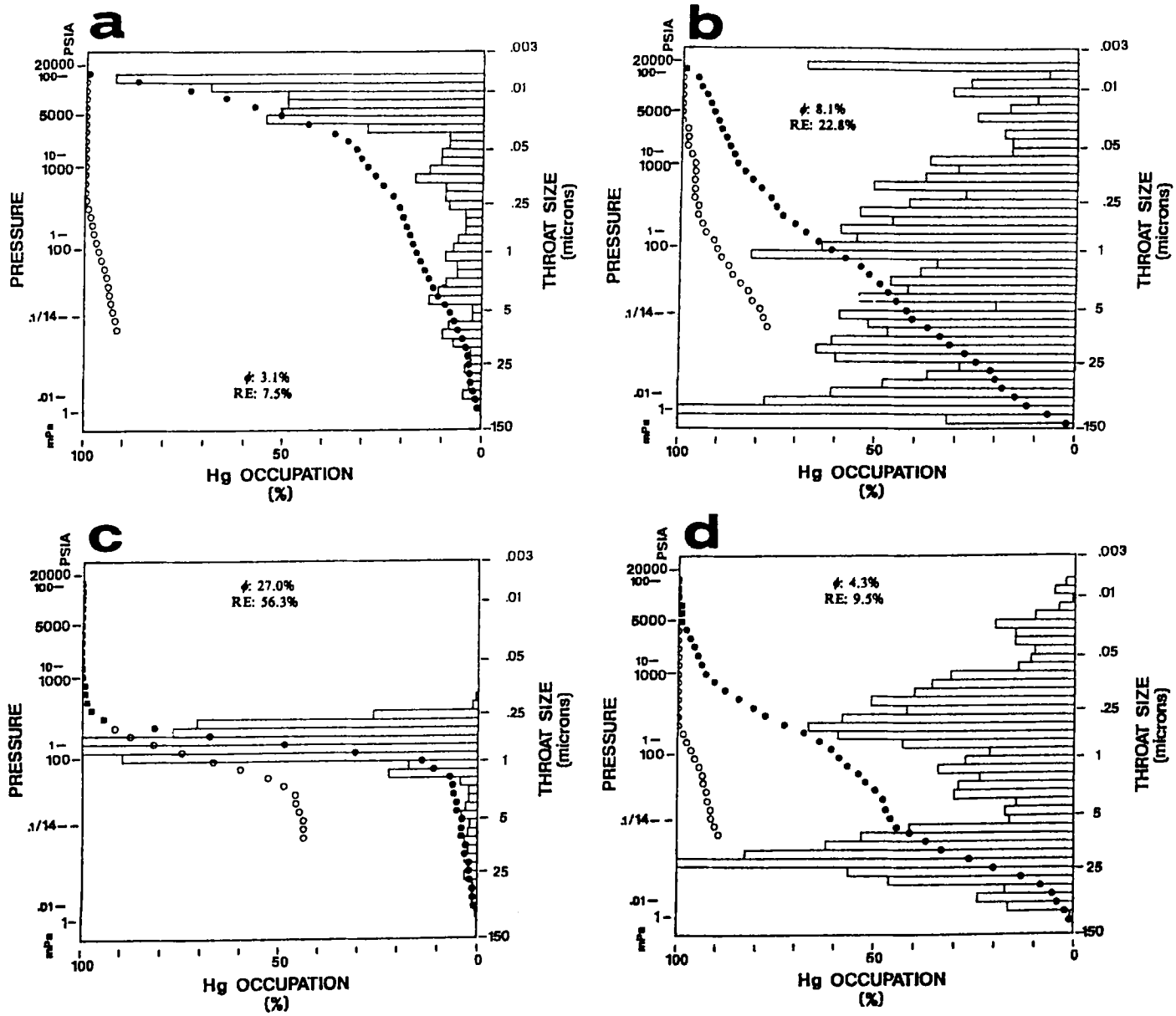

Figure 10. Capillary-pressure curves, Filled circles represent cumulative mercury intrusion; open circles extrusion; open bars of histogram are incremental intrusion. u: prosity; RE: recovery efficiency. a). Convex capillary-pressure curve of dolostone (Group D) from eastern Mediterranean. Graph shows low recovery efficiency and much more intrusion under high pressure than under low pressure. b). Gently sloping capillary-pressure curves of carbonate-cemented beachrock whose particles are mostly terrigenous (Group E) from Gulf of Elat, Red Sea. A similar quantity of intrusion occurred at both high- and low pressure. The RE and porosity are low. c). Intermediate capilary-pressure curves of pellet wackestone beachrock (Group C) from the Bahamas. It is characterized by good sorting of pore-throat size and large RE. The porosities of the rocks displaying this curve are high; of all the beachrocks studied, their petrophysical properties are the best. d). Bimodal capillary-pressure curves of carbonate-cemented beachrock whose particles are mostly terrigenous from Group E, Gulf of Elat, Red Sea. Incremental curve displays more than two peaks; such curves are for those samples having variable porosity and recovery efficiency.

median throat size and inversely proportional to RE, a finding in accordance with those of Wardlaw (1976, 1980).

These results also confirm that beachrocks (and possibly shallow-marine carbonates) are basically consolidated by cementation, and the effects of compaction can be ignored. Correspondingly, cementation, rather than compaction, controls the petrophysical properties of beachrocks. So rock age, which is often correlated with a rock's degree of compaction, does not determine the porosity in beachrocks.

4. Primary interparticle pores are the most-abundant type of pores in beachrocks. Dissolution vugs are not common. Intraparticle pores are very small and rare.

5. Most beachrocks show a positive relationship between porosity and RE, but oolite and Halimeda grainstones do not. Also, a rough positive relationship exists between porosity and median throat size. But recovery efficiency is inversely proportional to median throat size.

6. The dolostones from the Mediterranean exhibit peculiar petrophysical properties. Both porosity and recovery efficiency are very small, and the dolostones yield special, concave, capillary-pressure curves. These peculiarities could be the result of early diagenetic dolomitization in which most of the primary pores were lost.

ACKNOWLEDGEMENTS

Thanks are extended to Lillian Hess, Joachim Amthor, and David Kopaska-Merkel for help with the laboratory work. The manuscript was critically reviewed by David Kopaska-Merkel and John Sanders and edited by Steve Buttner. Their critical comments are deeply appreciated. Geochem Laboratories determined the radiocarbon ages. Reviewers Detlev K. Richter and Christian Strohmenger offered excellent suggestions which have been incorporated in this manuscript.

REFERENCES

AMIEUX, P., BERNIER, P., DALONGEVILLE, R., and MEDWECKI (de) V., 1989, Cathodoluminescence of carbonate-cemented Holocene beachrock from the Togo coastline (West Africa): an approach to early diagenesis: *Sedimentary Geology*, v. 65, P. 261-273.

AMTHOR, J. E., KOPASKA-MERKEL, D. C., and FRIEDMAN, G. M., 1988, Reservoir characterization, porosity, and recovery efficiency of deeply-buried (sic) Paleozoic carbonates: examples from Oklahoma, Texas, and New Mexico: *Carbonates and Evaporites*, v. 3, p. 33-52.

BATHURST, R. G. C., 1971, *Carbonate sediments and their diagenesis:* Amsterdam, Elsevier Pub. Co., 620 p.

BRICKER, O. P., ed., 1971, *Carbonate cements,* Baltimore and London, The Johns Hopkins Univ. Press, 376 p.

CHILINGAR, G. V., BISSELL, H. J., and WOLF, K. H., 1967, Diagenesis of carbonate rocks, p. 179-322, *in* Larson, G., and Chilinger, G. V. eds., *Diagenesis in sediments: Developments in Sedimentology 8:* Amsterdam, Elsevier Pub. Co., 572 p.

DULLIEN, F. A. L., and DHAWAN, G. K., 1974, Characterization of pore structure by a combination of quantitative photomicrography and mercury porosimetry: *Jour. Colloidal and Interface Science*, v. 47, p. 337-349.

DUNKEL, E., RICHTER, D. K., and SCHILLINGS, R. W., 1988, Aragonit versus Mg-Calcit-Zement in Holozänen Beachrocks der Perachora-Halbinsel (Korinth/Griechenland) als Ausdruck der Petrovarianz des Hinterlandes: *Bochumer geol. u. geotechn. Arb.*, v. 29, p. 40-42.

ETRIS, E. L., BRUMFIELD, D. S., EHRLICH, R., and CRABTREE, S.J., Jr., 1988, Relations (sic) between (sic) pores, throats and permeability: a petrographic/physical analysis of some carbonate grainstones and packstones: *Carbonates and Evaporites*, v. 3, p. 17-32.

FLÜGEL, E., 1982, *Carbonate microfacies:* Berlin, Springer-Verlag, 633 p.

FRIEDMAN, G. M., 1959, Identification of carbon-

ate minerals by staining methods: *Jour. Sed. Petrology*, v. 29, p. 87-97.

FRIEDMAN, G. M., and GAVISH, E., 1971, Mediterranean and Red Sea (Gulf of Aqaba) beachrocks: P.13-16 *in* Bricker, O. P., ed., *Carbonate cements:* Baltimore and London, the Johns Hopkins Univ. Press, 376 p.

FRIEDMAN, G. M., 1975, The making and unmaking limestones or the downs and ups of porosity: *Jour. Sed. Petrology*, v. 45, P. 379-398.

FRIEDMAN, G. M., and SANDERS, J. E., 1978, *Principles of Sedimentology:* New York, John Wiley and Sons, 768 p.

FRIEDMAN, G. M., RUZYLA, K., and REECKMANN, S.A., 1981, *Effects of porosity type, pore geometry and diagenetic history on the tertiary recovery of petroleum from carbonate reservoirs:* Rept. no. DOE/MC/11580-5, U.S. Dept. Commerce, U.S. Dept. of Energy: Springfield, Va., National Tech. Info. Service, 217 p.

FRIEDMAN, G. M., GHOSH, S. K., and URDSCHEL, S. 1990, Petrophysical characteristics related to depositional environments and diagenetic overprint: Mabee field, West Texas, *in* Bebout, D. G. and Harris P. M., ed., *Geologic and engineering approaches in evaluation of San Andres/Grayburg hydrocarbon Reservoirs-Permian Basin*, Bureau of Economic Geology, The University of Texas at Austin, P.125-144.

GAVISH, E., and FRIEDMAN, G.M., 1969, Progressive diagenesis in Quaternary to late Tertiary (sic) carbonate sediments: sequence and time scale: *Jour. Sed. Petrology*, v. 39, p. 980-1006.

GAVISH, E., and FRIEDMAN, G. M., 1973, Quantitative analysis of calcite and Mg-calcite by X-ray diffraction: effect of grinding on peak height and peak area: *Sedimentology*, v. 20, p. 437-444.

GHOSH, S. K., and FRIEDMAN, G. M., 1989, Petrophysics of a dolostone reservoir: San Andres Formation (Permian), West Texas: *Carbonates and Evaporites*, v. 4, no. 1, p. 45-119.

GINSBURG, R. N., 1953a, Beachrock in South Florida: *Jour. Sed. Petrology*, v. 23, p. 85-92.

HELSINGER, M. H., 1973 ms, Diagenetic modification and cementation at intertidal levels: Beachrock and oolite limestones from the Red Sea and Jamaica: Troy, New York, Rensselaer Polytechnic Institute, Master of Science Thesis, 126 p.

HELSINGER, M. H., and FRIEDMAN 1973, Diagenetic modification and cementation in carbonate sediments at intertidal levels (abstract): Geol. Soc. America, *Abstracts with programs*, v. 5, No. 2, p. 177.

ILLING, L. V., 1954, Bahaman calcareous sands: Am. Assoc. Petrol. Geol. Bull., v. 38, p. 1-95.

JENNING, J. B., 1987, Capillary pressure (sic) technique: Application to exploration and development geology, *Am. Assoc. Petrol. Geol. Bull.*, v. 71, p. 1195-1209.

KOPASKA-MERKEL, D. C., 1988, New applications in the study of porous media: determinations of pore-system characteristics on small fragments (part 1): *Northeastern Environ. Sci.*, v. 7, no. 2, p. 127-142.

KOPASKA-MERKEL, D. C. and AMTHOR, J. E., 1988, Very high-pressure mercury porosimetry as a tool in reservoir characterization: *Carbonates and Evaporites*, v. 3, p. 53-64.

KOPASKA-MERKEL, D. C. and FRIEDMAN, G. M., 1989, Petrofacies analysis of carbonate rocks: Example from the Lower Paleozoic Hunton Group of Oklahoma and Texas: *Am. Assoc. Petrol. Geol. Bull.*, v. 73, p. 1289-1306.

KRUMBEIN, W. E., 1979, Phytolithotropic and chemoorganotrophic activity of bacteria and algae as related to beachrock: *Geomicrobiology Journal*, v. 1, no. 2, p. 139-203.

MEYERS, H.M., 1987, Marine vadose beachrock cementation by cryptocrystalline magnesian calcite--Maui, Hawaii: *Jour. Sed. Petrology*, v. 57, p. 558-570.

MILLIMAN, J. D., 1974, *Marine Carbonates:* Berlin, Springer-Verlag, 375 p.

MÜLLER, G., 1967, *Methods in sedimentary petrology:* New York, Hafner Pub. Co., 283 p.

MÜLLER, G., and Gastner, M., 1971, The "Karbonat-Bombe", a simple device for the determination of the carbonate content in sediments, soils and other materials: *Neues Jahrbuch Mineral. Mh.*, no. 10, p. 446-469.

PURCELL, W. R., 1949, Capillary pressures--their measurement using mercury and the calculation of permeability therefrom: *American Institute of Mining, Metallurgical, and Petroleum Engineers, Petroleum Transactions.* v. 186, p. 39-48.

RUSSELL, R. J., 1963, Beachrock: *Journal Tropical Geography,* v. 17, p. 24-27.

SCHILLINGS, R. W., and RICHTER, D. K., 1989, Rezente Beachrockbildungen an den Küsten Griechenlands: Geol. Paläont. Mitt. Innsbruck, Bd. 16, p. 96-98.

SCHOWALTER, T. T., 1979, Mechanics of secondary hydrocarbon migration and entrapment: *Am. Assoc. Petrol. Geol. Bull.*, v. 63, p. 723-760.

STODDART, D. R., and CANN, J. R., 1965, The nature and origin of beachrock: *Jour. Sed. Petrology,* v. 35, p. 243-247.

TAYLOR, J. C. M., and ILLING, L. V., 1969, Holocene intertidal calcium carbonate (sic) cementation, Qatar, Persian Gulf, p.68-108, *in* Füchtbauer, H., ed., *Lithification of carbonate sediments 1. Sedimentology,* Amsterdam, Elsevier Pub. Co., 160 p.

WARDLAW, N. C., 1976, Pore geometry of carbonate rocks as revealed by pore casts and capillary pressure: *Am. Assoc. Petrol. Geol. Bull.*, v. 60, no. 2, p. 245-257.

WARDLAW, N, C., and TAYLOR, R. P., 1976. Mercury capillary pressure curves and the interpretation of pore structure and capillary behavior in reservoir rocks: *Bull. Can. Petrol. Geol.*, v. 24, p. 225-262.

WARDLAW, N. C., 1980, *The effects of pore structure on displacement efficiency in reservoir rocks and in glass micromodels:* SPE AIME, Symp. on Enhanced Oil Recovery, Tulsa, Preprint SPE 8843, p. 345-352.

WARDLAW, N. C., and MCKELLAR, M., 1981, Mercury porosimetry and the interpretation of pore geometry in sedimentary rocks and artificial models: *Powder Tech.*, v. 29. p. 127-143.

WARDLAW, N, C., MCKELLAR, M., and YU, LI, 1988, Pore (sic) and throat size (sic) distribution determined by mercury porosimetry and by direct observation: *Carbonates and Evaporites,* v. 3, p. 1-16.

Manuscript received
Manuscript accepted